第 48 卷 第 12 期
2021 年 12 月

湖南大学学报（自然科学版）
Journal of Hunan University (Natural Sciences)

Vol. 48 No. 12
December 2021



# Challenges of Acquisition Bathymetry Information on PlanetScope Data and Nautical Chart: Experiment Based on IHO S-44 Total Vertical Uncertainty in Multi-Method Satellite-Derived Bathymetry

**Agung Kurniawan[1,2]*, Widodo Setiyo Pranowo[2,4]*, Yosef Prihanto[3], Avando Bastari[4], Johar Setiyadi[4]**

[1] Geographic Information System, Department of Geo-Informatics, Vocational College, Universitas Gadjah Mada, Yogyakarta, Indonesia

[2] Marine and Coastal Data Laboratory, Marine Research Center, The Republic of Indonesia Ministry of Marine Affairs & Fisheries, Jakarta, Indonesia

[3] Indonesian Geospatial Information Agency, Bogor, Indonesia

[4] Indonesian Naval Postgraduate School (STTAL), Jakarta/Surabaya, Indonesia

**Abstract:** Regular depth data monitoring is an essential element in navigation or non-navigation. As the primary information in creating navigation maps, depth data can be obtained immediately without direct field measurements using a remote sensing method called Satellite-Derived Bathymetry (SDB). However, the method has weaknesses, especially in the accuracy level. This study aims to obtain bathymetric information from three methods with different characteristics and to compare the accuracy of the three methods that are best suited to the conditions of the research area. Experiments were carried out by adopting Stumpf, Global, and Single Band comparable SDB methods. The three methods use simple statistical linear regression involving the visible band and band ratio. Tidal events are also considered in the SDB extraction process as a parameter for water level correction. This research was conducted on Johnston Atoll Island, a remote area in the Pacific, specifically located in the northwest of the Hawaiian Islands. The accuracy calculation was based on Root Mean Square Error (RMSE) and Total Vertical Uncertainty (TVU), referring to International Hydrographic Organization (IHO) S-44. This study chose TVU because it complies with IHO recommendations and standards. The use of TVU to see the accuracy of the bathymetric model results becomes important as part of the implementation of IHO standardization. The SDB experiment results were normalized and corrected to low tide to obtain a depth close to the actual value and eliminate the tidal effect. The results showed that the RMSE with the Stumpf and Global methods increased systematically. A systematic decline involved adopting the single band method by increasing depth class with the most optimal results. By adopting the Stumpf Method, the accuracy of the experimental results based on TVU was 19.4% collectively for the depth range of 10.01-20 meters. However, the accuracy of the single band method was 28.2% and 16.5% for the 0–5- and 5.01-10 meter depth ranges, respectively.

**Keywords:** satellite-derived bathymetry, remote area, root mean square error, total vertical uncertainty.

# 在行星範圍數據和海圖上獲取水深信息的挑戰：基於國際水文組織 S-44 多方法衛星測深中總垂直不確定度的實驗

**摘要：**定期深度數據監測是導航或非導航的基本要素。作為創建導航地圖的主要信息，深度數據可以立即獲得，而無需使用稱為衛星測深的遙感方法直接進行現場測量。然而，該方法有弱點，特別是在準確度水平上。本研究旨在從具有不同特徵的三種方法中獲取測深信

Received: August 13, 2021 / Revised: October 16, 2021 / Accepted: November 18, 2021 / Published: December 30, 2021

About the authors: Agung Kurniawan, Geographic Information System, Department of Geo-Informatics, Vocational College, Universitas Gadjah Mada, Yogyakarta, Indonesia; Marine and Coastal Data Laboratory, Marine Research Center, The Republic of Indonesia Ministry of Marine Affairs & Fisheries, Jakarta, Indonesia; Widodo Setiyo Pranowo, Marine and Coastal Data Laboratory, Marine Research Center, The Republic of Indonesia Ministry of Marine Affairs & Fisheries, Jakarta, Indonesia; Indonesian Naval Postgraduate School (STTAL), Jakarta/Surabaya, Indonesia; Yosef Prihanto, Indonesian Geospatial Information Agency, Bogor, Indonesia; Avando Bastari, Johar Setiyadi, Indonesian Naval Postgraduate School (STTAL), Jakarta/Surabaya, Indonesia
Corresponding authors Agung Kurniawan, agung.kurniawan.16@mail.ugm.ac.id; Widodo Setiyo Pranowo, widodopranowo@gmail.com

息，並比較最適合研究區域條件的三種方法的準確性。通過採用斯坦普夫、全局和單波段可比 衛星測深 方法進行實驗。這三種方法使用簡單的統計線性回歸，涉及可見帶和帶比。在衛星測深 提取過程中，潮汐事件也被視為水位校正的參數。這項研究是在太平洋偏遠地區約翰斯頓環礁島上進行的，特別是位於夏威夷群島西北部。精度計算基於均方根誤差和總垂直不確定度，參考國際水文組織小号-44。本研究之所以選擇 總垂直不確定度，是因為它符合國際水文組織 的建議和標準。作為國際水文組織標準化實施的一部分，使用 總垂直不確定度查看測深模型結果的準確性變得很重要。將 衛星測深 實驗結果歸一化併校正到低潮，以獲得接近實際值的深度並消除潮汐效應。結果表明，使用斯坦普夫和全球的方法的根均方誤差系統地增加了。系統性下降涉及通過增加深度等級來採用單波段方法，以獲得最佳結果。採用斯坦普夫方法，基於 總垂直不確定度 的實驗結果在 10.01-20 米深度範圍內的準確率為 19.4%。然而，對於 0-5 米和 5.01-10 米深度範圍，單波段方法的準確度分別為 28.2% 和 16.5%。

**关键词**：衛星測深、偏遠地區、均方根誤差、總垂直不確定性。

## 1. Introduction

Coastal areas are dynamic environments that transform rapidly due to climate change in the oceans that could be influenced by various anthropogenic processes and global climate [1]. For this reason, later marine space mapping applications require more comprehensive bathymetric data, leading to increased demand for detailed bathymetry and diversifying data collection techniques. Furthermore, the need for seabed topographical information encourages the development of more flexible bathymetry acquisition techniques by utilizing the existing ship and space platforms [2]. Accurate bathymetric modeling is required for safe marine navigation in shallow water areas or other operations [3]. In general, accurate and regularly updated coastal bathymetry information is essential for studies on the marine environment [4].

Periodic monitoring of depth data for navigation and non-navigation in a water area makes bathymetric data expensive and requires a long acquisition period [5]. As the main information for making navigation maps, depth data could be obtained efficiently without direct field measurements using a remote sensing method called Satellite-Derived Bathymetry (SDB). This approach assumes that the deeper water is darker than, the shallower one (water clarity) [6, 7], as illustrated in Fig. 1. Moreover, the SDB method is a major tool in global shallow-water monitoring at a relatively low cost [8, 9].

Shallow waters capture the sun's radiation more optimally, and the information is recorded by remote sensing satellites (see Fig. 1). They are characterized by the bottom of the water (and the substrate composition), which is visible and objectively captured by satellite sensors. In contrast, waters between shallow and deep could still be visually observed by the water column but cannot penetrate to the bottom. The last category is deep water, into which light cannot penetrate, and the satellite sensor is depicted in a dark hue, indicating no information obtained through visual analysis. The concept of solar radiation infiltration to the water column is important in applying the Satellite-Derived Bathymetry method. Johnston Atoll Island is a remote island in the Pacific Ocean often used for pilot projects or international research experiments as a benchmarking method [10]. The sea waters around this island are clear, and the coastal gradient forms an ideal morphology from shallow to deep waters. The island is located in the middle of the Pacific Ocean, adjacent to the Hawaiian Islands, and is one of the outermost islands of the USA.

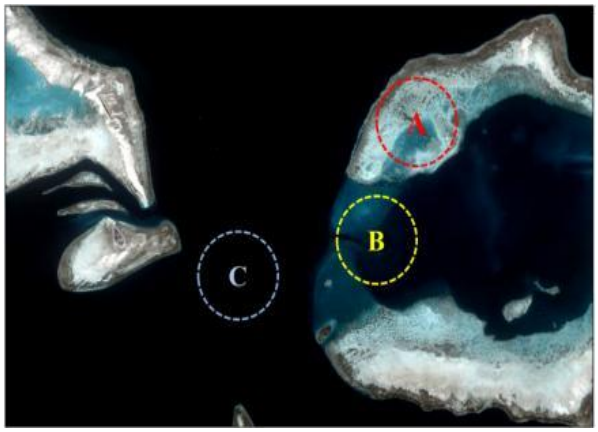


Fig. 1 Differences in water hue due to solar radiation infiltration: A) Shallow-water; B) Waters between deep and shallow, and C) Deep waters, where the water fully absorbs sunlight

The location of this island is seen clearly in Fig. 2. Directly facing the high seas, Johnston Atoll Island is

vulnerable to in-depth information changes due to the ocean wave dynamics, intervention from the mainland, and climate change. Therefore, comprehensive research on the bathymetric data acquisition accuracy using remote sensing is essential for this island. The SDB method was chosen due to its relatively cheap and fast operational cost in remote areas.

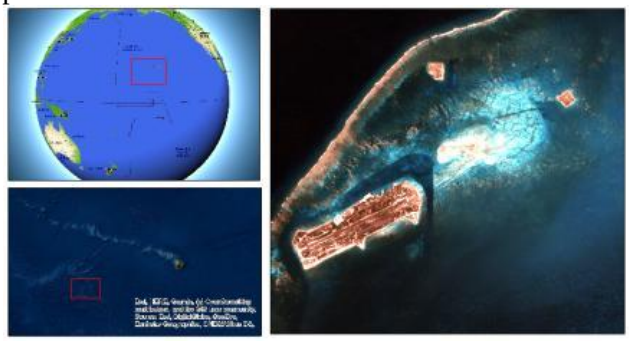

Fig. 2 Relative Location of Johnston Atoll Island in the Pacific Ocean (taken from Google Earth Collection, ESRI Imagery, and Planet Scope 3B)

This study compared three methods to obtain bathymetry data using satellite data. All methods, including Stumpf, Global model, and Single Band, employed empirical approach models and considered the parameters of tidal events. SDB's rapid development enhances mapping and shipping navigation, especially in shallow waters far from the mainland. Based on these conditions, the data from the SDB results need adjustment to the survey standard from the IHO, known as TVU (Total Vertical Uncertainties). According to the United Kingdom Hydrography Office (UKHO), good quality SDB data is useful as valid supporting information and essential in securing navigation products [11]. The use of TVU is essential to see the ability of the resulting SDB to meet the standards set by IHO.

## 2. Scope, Materials, and Methods

### 2.1. Satellite-Derived Bathymetry and International Regulations

Depth estimation algorithms based on optical satellite digital images are categorized into physics-based and empirical models (EMs) [12, 4]. The SDB method using the empirical approach assumes that atmospheric conditions do not change. Therefore, the model could be generalized to all images and depth layers produced with acceptable accuracy. However, it has limitations due to different conditions of satellite imagery in each scene. Consequently, the depth information survey results are still required even when limited due to the quality control of image data and the extraordinary experience of the analysts to cover three or more areas of hydrography, cartography, and GIS. In empirical modeling, the relationship between remote sensing emission and depth is determined empirically by ignoring the light propagation infiltration process.

Furthermore, the correlation between water depth and spectral band radiation is used to calculate SDB. This modeling assumes that the total reflectance is mainly related to water depth and secondary turbidity. Empirical parametric regression-based models, such as Stumpf et al. [26], are popular methods. This model allows fast data extraction but requires depth point calibration [9].

The empirical approach assumes that light is attenuated exponentially with depth through the water surface and depends on the level variation for light at different wavelengths to estimate the water depth. Additionally, the attenuation coefficient is unknown and derived empirically through band ratio regression on in situ depth data. The empirical study considers that the attenuation ability at each depth is the same in the whole image. The SDB satellite image is multispectral and accommodates visible channels for green and blue. The infiltration of solar radiation is optimal in these two channels. Satellite imagery is available in various spatial resolutions (+ 100m to 31cm). SDB is only applied to images with a spatial resolution higher than 30m. However, they are suitable for marine mapping applications since SDB produces an average depth per pixel. Even when using images with a spatial resolution of 30 m, the results must be used with caution due to the many potential undetected depths. Conversely, images with higher resolutions with black and white wavelengths cannot be extracted for depth information and purposes [13].

IHO standardization has an accuracy assessment method known as TVU (Total vertical uncertainty). It is a one-dimensional quantity that includes all contributions to the vertical measurement uncertainty [14]. Furthermore, TVU and total horizontal uncertainty are the International Hydrographic Organization (IHO) reference standards used for quality and uncertainty assessment for hydrographic survey activities [1]. The two main properties contributing to TVU based on SDB are uncertainty regarding the radiometric characteristics of the satellite imagery and screening process and the quality of control points. Therefore, it is assumed that the uncertainties of the two key properties are independent and could be approximated as Gaussian variables [15]. TVU was used to evaluate the vertical accuracy of water depth from in-situ data and was estimated using equation (1).

Additionally, the maximum allowable horizontal uncertainty (THU/Total horizontal uncertainty) from in-situ data at a 95% confidence level was taken 2 m away. In situ bathymetric data meet the IHO standard uncertainty requirements for special order hydrographic surveys. The a and b in equation (1) are 0.25 m and 0.0075, respectively (Table 1).

$$TVU = \pm\sqrt{a^2 + (b \times d)^2} \quad (1)$$

where:

$a$ is the uncertainty portion that does not vary with the depth;

*b* is a coefficient representing the uncertainty portion that varies with the depth;
*d* is the depth.

Table 1 IHO S-44 maximum allowable uncertainties based on IHO S-44 survey standards [10]

| Order of survey | Maximum allowable TVU |
|---|---|
| Special | *a*: 0.25 *b*: 0.0075 |
| 1a | *a*: 0.5 *b*: 0.013 |
| 1b | *a*: 0.5 *b*: 0.013 |
| 2 | *a*: 1 *b*: 0.023 |

## 2.2. Concept of Sun Radiation Infiltration to Water

Remote sensing-based bathymetry is developed because the total radioactive energy reflected from the water column represents the actual depth of water. Specifically, the optical system remote sensing utilizes short-wave radiation in the blue and green spectrum, with a fairly high infiltration capability. The solar radiation penetrating water is scattered and absorbed by water molecules and constituents, leaving energy reflected in the remote sensor. The sensor receives energy that describes the reflection from the water column to the bottom of the optically shallow seawater. Moreover, light entering the water column is absorbed and scattered from the water body and the substrate (Fig. 3). Light energy is greatly attenuated as it enters deeper water due to absorption by water molecules, dissolved substances, or particles (organic and inorganic) and the scattering of suspended particles [16].

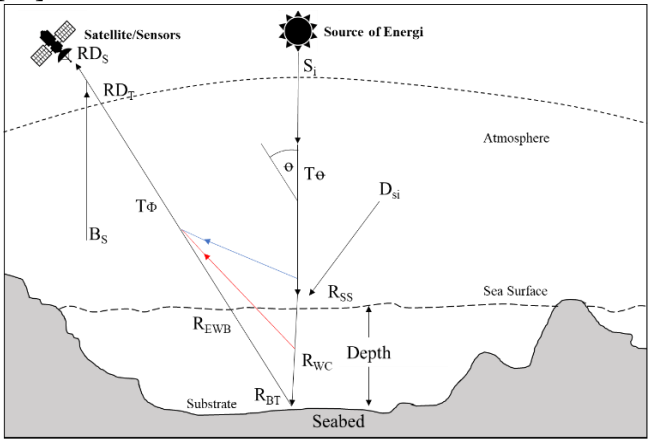


Fig. 3 The scheme of sunlight infiltration into water bodies in shallow water, the sunlight passes through several obstacles before reaching the bottom. It influences radiance before reaching sensors (Modified from [16])

[16] stated that the barriers in this scheme are described as follow:

($S_i$) - solar illumination top of the atmosphere;
($T\Phi$ $T\square$) - atmospheric transmittance;
($D_{si}$) - diffuse sky irradiance;
($R_{SS}$) - reflectance from the sea surface;
($R_{WW}$) - reflectance in the water column, including molecules and particles;
($R_{BT}$) - reflectance from the shallow water floor or substrate;
($R_{EWB}$) - effective reflectance from the water body (not including $R_{SS}$);
($B_p$) - back-scatter;
($RD_T$) - the target radiation transmitted by the atmosphere;
($RD_S$) - radiation received at the sensor.

The deeper the water, the more solar energy is restrained due to light absorption by water molecules, solutes, or organic and inorganic particles. Additionally, the scattering of suspended particles prevents sunlight from entering the bottom of the water. Theoretically, the sunlight infiltration into water is a basic assumption for making shallow bathymetry models using several parameters simulated with statistics. It aims to determine the best parameter combination, especially for satellite-derived bathymetry, which assesses the relationship between empirical depth and pixel values [17]. In defining a bathymetric model, Jupp [27] used the basic principle that radiation is attenuated at different wavelengths and rates as it penetrates the water column. The water column depth penetrable by light and recorded by a sensor wavelength is called the DOP (Depth of Penetration), which must be calibrated to obtain a rational value in the algorithm [18]. Each channel has a different DOP depth (see Fig. 4).

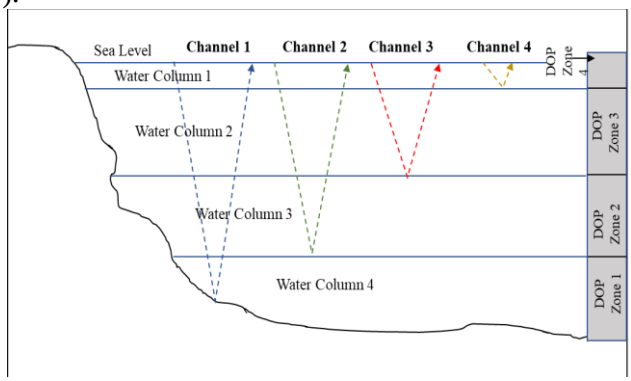


Fig. 4 Depth of penetration (DOP) zone by each band/channel

The Depth of Penetration (DOP) calculation results show that depth interpolation in the penetration zone is conducted to obtain a depth calibration. Therefore, this method is developed because radiance is attenuated at different rates to penetrate the water body [17].

## 2.3. Materials and Data

The primary data used in this research is PlanetScope multispectral satellite imagery, with a resolution of 3.5 meters. The image was recorded through 3 FOV (Field of View) scenes on 30 October 2020 (see Fig. 5a). Furthermore, image selection was based on cloud-free image characteristics to avoid interfering with the algorithm. The planet scope used an image corrected to level 3B, cartographically projected, and radiometric correction to the SR (Surface Reflectance) level [19].

The depth extraction was performed using the SDB method and empirical approach, meaning that a depth sample is still needed to make a "presumption" of the whole. Moreover, depth data were obtained from NOAA marine map number 83637 plan B, covering Johnston Island and its surroundings (Fig. 5b) with a depth range from 0.9 m to 20 m. The result of depth extraction on the SDB method is a "raw" depth that needs adjustment to the tidal conditions and the area's dynamics. Tidal data is needed to correct and obtain the actual depth extracted data (SDB) using tidal observation data for 31 days. The data correction was due to the influence of tidal depth dynamics during image recording, resulting in biased results.

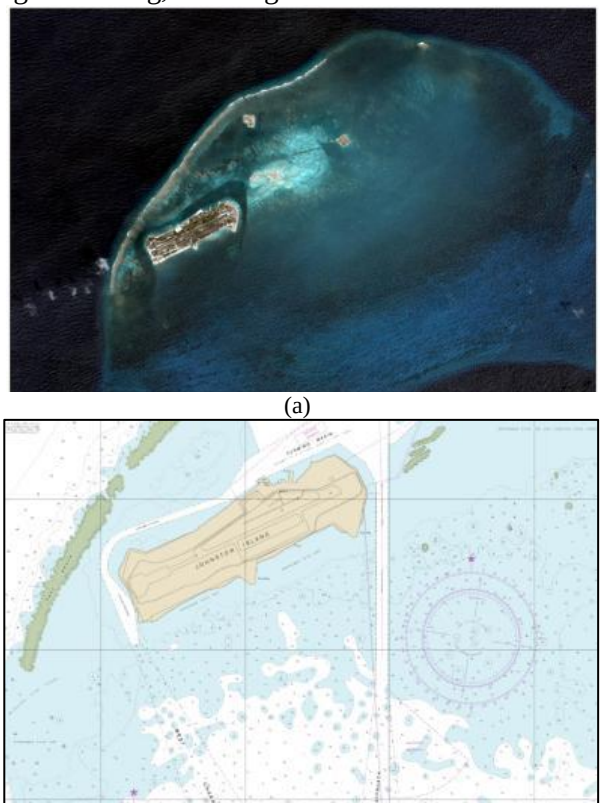

(a)

(b)

Fig. 5 PlanetScope Multispectral Image with 3meter spatial resolution and four channels (Red, Greem, Blue, NIR) (a); NOAA Nautical Chart number 83637 plan B, Johnston Atoll waters (b)

Satellite imagery obtained was PlanetScope, with data level 3B or analytical, indicating that the image was processed on the Ortho-Scene Product with four multispectral channels (see Table 2). This image was obtained through the Planet Education and Research program. Moreover, level 3B indicates that the image was orthorectified, and the pixel value was converted at the Surface Reflectance level. PlanetScope satellite images at level 3B were projected into the Universal Transverse Mercator cartographic projection for each image scene [20].

The entire Johnston Atoll was covered using three image scenes recorded on 30 October 2020 and radiometrically corrected using sensor telemetry and models. Furthermore, the image was corrected geometrically using ground control points (GCPs), a fine digital elevation model with a resolution of 30-90 m, and projected onto a cartographic projection, such as UTM WGS84. Atmospheric effects were then recorded using the radiative transfer code 6SV2.1. Input AOD, water vapor, and ozone were taken from MODIS images in real-time [21].

Table 2 Multispectral channel information and proprietary resolution [19]

| Band | Wavelength | Spatial Resolution |
|---|---|---|
| Blue | 455 – 515 nm | |
| Green | 500 – 590 nm | 3 meters |
| Red | 590 – 670 nm | |

## 2.4. Tides Processing

The tide is an important component in obtaining depth information via Satellite-Derived Bathymetry (SDB). Tidal correction is conducted to eliminate effects occurring when recording satellite image data, using configuration from 1 October to 31, 2020, indicating the data is the 30th day + 1. The data was processed using MIKE 21 Toolbox [22] and 36 tidal harmonic constants obtained from NOAA's official website [28]. The following information was obtained in tidal processing:

- Sea level datum (S0) or calls as mean sea level (S0) is the position calculated by averaging the tidal observation results arithmetically, using the following equation:

$$Temporary\ MSL = \frac{\sum(\text{Water level x Constituent})}{\sum(\text{Constituent})} \quad (5)$$

- The tidal harmonics constant is applied to assess the generating component of the tides due to the moon and sun movement towards the earth. It consists of 36 constants [28].
- The Tidal Property defines tidal events in a certain area using the Formzahl Equation.

$$F = \frac{A(K_1 + O_1)}{A(M_2 + S_2)} \quad (6)$$

- *Chart Datum* ($Z_0$) is a low water position, and there is rarely a receding value below the datum chart position.

$$Z_0 = \sum_{i=1}^{n} A_i \quad (7)$$

- *Depth Reduction* is calculated by finding the difference between the sea elevation and the chart datum value during image recording.

$$\text{Reduction value} = Z_t - \text{Chart datum} \quad (8),$$

where:

$Z_t$ - sea elevation on *Tide pole.*

- The tidal correction was carried out to obtain the actual depth of the SDB extraction results.

$$Z = Z_i - \text{Reduction value} \quad (9),$$

where:

$Z$ - Actual depth value;

$Z_i$ - depth value from SDB result.

To facilitate understanding the tidal correction principle, Fig. 6 illustrates the tide components used to correct the depth generated from the SDB.

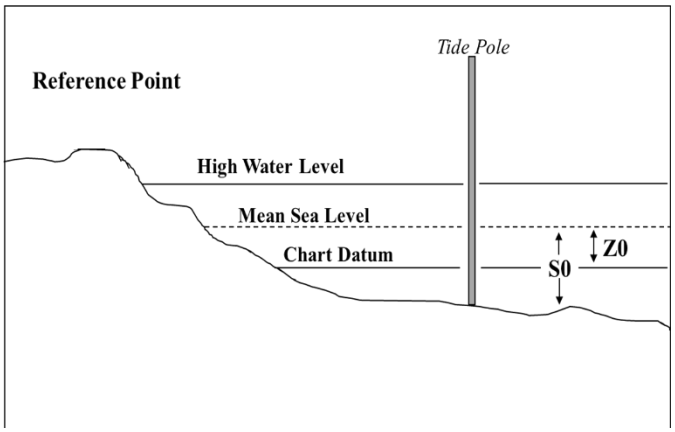


Fig. 6 Theoretical illustration of tidal component positions for ocean depth analysis

### 2.5. Deriving Depth Using Stumpf Algorithm

The model from Stumpf et al. [26] was developed using the basic principle of absorption rate of water bodies conveyed by each channel. The diverse absorption of water bodies theoretically produces a ratio between bands. The ratio then produces a simultaneous change with the depth [2]. This method is characterized by the relationship between the remote sensing reflectance ratio above the water surface and the two bands to a priori water depth [23]. Each band has a different absorption level. Conceptually, this difference produces a ratio between bands and changes with depth.

The log-transformed relationship between the ratio bands with higher lower absorption was derived. Theoretically, increasing the ratio increases the depth. Therefore, the band with a higher absorption rate decreases as the depth increases, and a linear model is developed between the ratio and the retrieved water depth [2, 23]. This log-ratio model is more potent with accurate depth estimation, especially for shallow habitats with low reflectance and deeper benthic habitat areas than other derived models [23]. The equation used to obtain SDB in the Stumpf et al. [26] algorithm is as follows:

$$Z = m_1 * \frac{\ln(nR\ (\lambda i))}{\ln(nR\ (\lambda j))} - m_0 \qquad (10)$$

where:
$m_1$ - tunable constant to scale the ratio to the depth;
N - a fixed constant for all areas;
$m_0$ - the offset for a depth of 0 m (Z = 0).

### 2.6. Deriving Depth Using Global Regression Analysis

Global Regression Analysis or model uses coefficients to make predictions [24]. The model equation is obtained through linear regression to the appropriate calibration point. Additionally, it generates coefficients and equations to obtain the Z depth value for pixels at other positions in the image. The calibration point test set is used to test the fit in this regression. These equations then generate bathymetric models, which are further processed (smoothing, contouring, pseudocolored) according to the required application. In the global model, the depth derived from the sample data is considered the dependent variable, while the transformed radian (X(λ)i) is the independent variable for calculating the regression coefficient [24].

$$D = \beta_0 + \beta_1(\lambda)_1 + \beta_2(\lambda)_2 + \cdots + \beta_n(\lambda)_n \qquad (11)$$

Coefficient $\beta$ is derived from multiple linear regression with depth from depth data, where D is the approximate depth, $\beta_0$ represents the y-intercept, and $\beta_1, \beta_2 \ldots \beta_n$ are the slope for each channel. According to [24], the value of $(\lambda)_i$ is reflectance transformation. However, it is ignored in this study due to the visual separation of the optical shallow and deep-sea, avoiding bias due to missing pixel values. In order to determine coefficients and estimate bathymetry, samples at depth points were obtained from randomly distributed data sources [5, 24, and 17].

### 2.7. Single Band Method

The bathymetric model constructed through empirical modeling involves a single band in the visible channel in the PlanetScope imagery. Technically, the energy propagating in the water column is attenuated in this method and decreases as the depth increases. Additionally, longer waves are attenuated more strongly than shorter wavelengths. Crucial considerations in using this single band method are variations in depth of the study area, band selection, and attenuation characteristics of the water column. Furthermore, the most effective bands in bathymetric modeling consider depth variations because they relate to how fast the energy is attenuated to the bottom of the water. Bathymetric modeling is run in case of a significant difference between pixel values due to differences in water depth.

### 2.8. Image Processing: Land and Water Body Separation

The depth extraction through the SDB process only requires aquatic objects, especially shallow waters. For this reason, water and land areas are separated using the NIR channel (see Fig. 7a). Moreover, the land pixel value is removed based on the meeting point of land and water (see Fig. 7b). A line was interpolated on the satellite image's near-infrared band (Fig. 10a) to extract a threshold value. It separates the land and water pixels for the blue and green bands. Both pixels are easily identified in the near-infrared image—the smooth (fluctuating) region with low values represents water instead of high values for land [1].

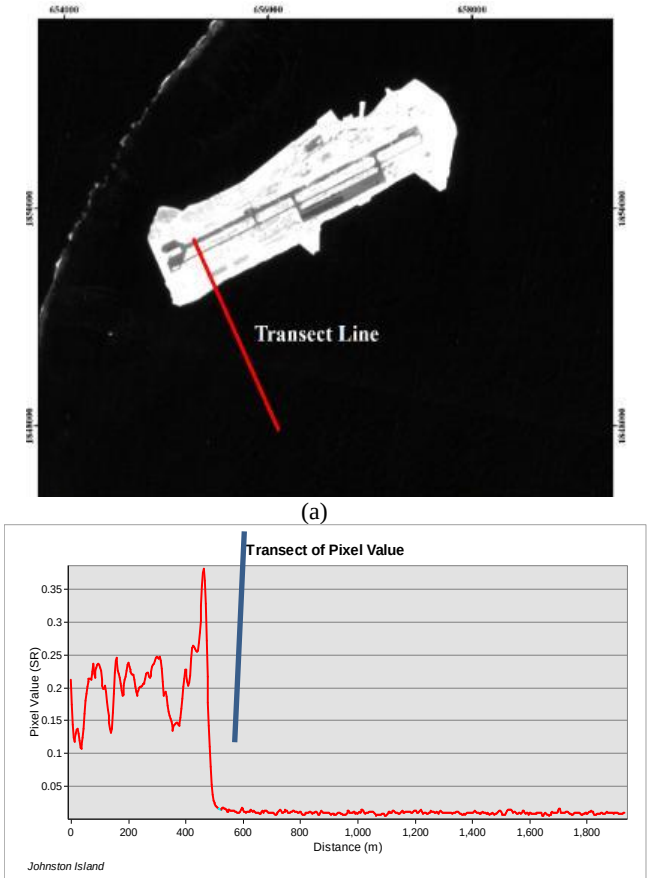


(a)

(b)

Fig. 7 Threshold values extracted from the near-infrared (NIR) band from the transect line (a). The interpolated line indicates the area on which offshore and onshore reflectance values were extracted, as presented on the profile. Constant and low values indicate water pixels, while high and fluctuant values indicate land pixels (b)

# 3. Results

## 3.1. Tides Processing Result

The tidal station used as a benchmark has a code of 1619000 (Johnston Atoll). Water level information was obtained through a prediction process using MIKE 21 software [30], utilizing tidal harmonic constants in Johnston Atoll waters [28]. Observations of water level conditions for 29 days and tidal prediction data show a mixed tidal dynamic around the area, leaning to double with a value of 0.26016. This figure is obtained through the Formzahl Equation (see Fig. 8a). Moreover, the first category obtained is MSL/S0 (temporary) to determine sea-level position. Due to this temporary characteristic, the datum was calculated using a constellation of three continuous tidal days, based on the tidal phenomenon from 29 October 2020 to 1 November 2020. The value obtained for the temporary MSL based on an average calculated for three days is 93.3 cm from zero palms. The temporary MSL calculated based on tidal phenomena from 29 October 2020 to 1 November 2020 is shown in the graph in Fig. 8 b.

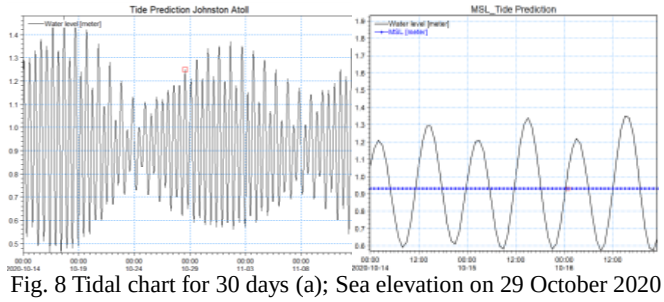


Fig. 8 Tidal chart for 30 days (a); Sea elevation on 29 October 2020 – 1 November 2020 for temporary MSL calculations (b)

The chart datum obtained from the information on the map was measured accurately and precisely. The calculation results show that the tidal character around Johnston Atoll water is Mixed Tide Prevailing Semi Diurnal. The difference between the water level during image recording and the datum chart determines the depth reduction value in this study (see Table 3). Subsequently, the depth reduction is substantial to obtain the actual bathymetry depth processed by Satellite-Derived Bathymetry.

Table 3 Calculation of chart datum, tidal properties, and chart datum

| Tidal type | Chart datum ($Z_0$) | Sea elevation from satellite imagery | Depth reduction |
|---|---|---|---|
| 0.31 (mixed tide prevailing semi diurnal) | 30.5 cm | 100 cm | 69.5 cm |

## 3.2. SDB Processing Result

Land and water separation is the first step in deriving bathymetry data from satellite imagery. A pixel value represents each smallest object in the image that the sensor could record. Also, the threshold value between water and land (see Fig. 6b) is the basis for separating land from water. The image pixel values more than 0.0596 are deleted automatically, leaving pixels in the water area (see Fig. 9). Referring to the algorithm Stumpf [26] developed in equation 10, the band ratio is obtained by dividing the blue and green bands. This ratio model is made to produce a linear response with depth and to evaluate the empirical solution.

Furthermore, it is applied to equation 8 to obtain and estimate the depth value. The ratio process results in a narrower range of numbers for their pixel values and no longer represents the true depth. For this reason, it becomes the basis for continuing the processing to information reduction in Satellite-Derived Bathymetry.

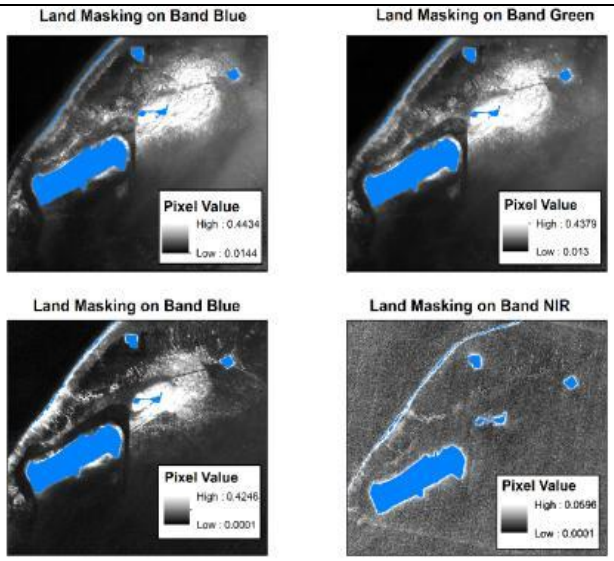


Fig. 9 Separation of land and water objects based on pixel values

The combination of depth data and ratio values is used for the regression process, resulting in the variables $m_1$ (tunable constant to scale the ratio to depth) and $m_0$ (the offset for a depth of 0 m). Additionally, the regression calculation obtained a coefficient of determination ($R^2$) of 0.6305. Therefore, the pixel value in the ratio image (X1) affects the depth level of up to 63.05%, implying a negative relationship between the pixel value in the ratio image and the depth level. The decrease in the pixel value in the ratio image (X) increases the depth level (Y) (see Fig. 10a). The sample distribution is shown in Fig. 10(b). The results of each stage of SDB processing using the Stumpf method on Johnston Atoll water are presented in Fig. 11.

The original SDB processing using the Stumpf method [26] in Johnston Atoll waters resulted in a depth ranging between 33.0242 and 13.9397 meters (in positive condition) (see Fig. 11a). Subsequently, a normalization process was carried out to obtain a more rational figure representing the height in the intertidal region (-0.00014028 - 0 meters) with waters (0 - 33.0242 meters) (see Fig. 11b). The numbers are set in a positive condition for ease of calculation in the initial processing. Also, it represents the sample data taken as positive numbers (float). The SDB is then corrected using the tidal value to eliminate the tidal effect (Fig. 11c). Furthermore, the depth value is changed to negative to adjust the water conditions to the real states (positive refers to intertidal and negative implies depth) (Fig. 11d).

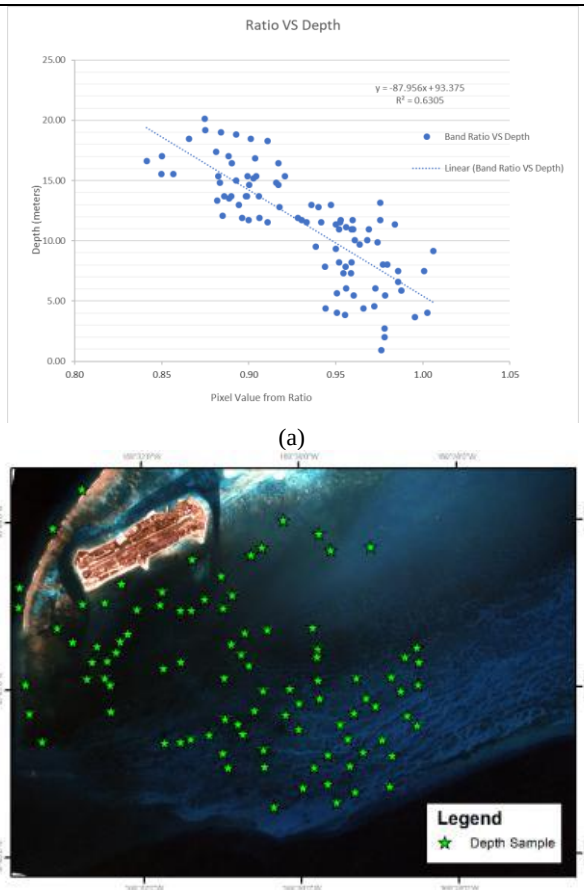


Fig. 10 Regression result graph showing the relationship between the pixel band ratio value and depth (a); distribution of the depth sample used (b)

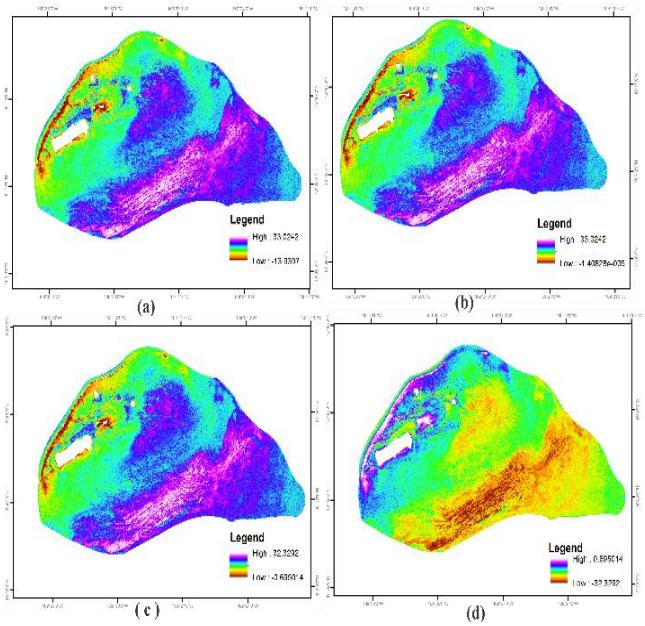


Fig. 11 Original SDB processed by Stumpf method (a); The normalized SDB results (b); SDB corrected by the tide (c); SDB whose depth value has been adjusted to below the water level (minus) (d)

According to the pixel dimensions, the resulting depth is obtained based on the predicted pixel value transformation using a regression scheme. In this case, the spatial resolution of the PlanetScope satellite image is 3 x 3 meters, representing the depth within that area

(see Fig. 12), resulting in high depth complexity. Fig. 13 shows a depth profile, where the resulting graph is a transect depiction of the seabed surface.

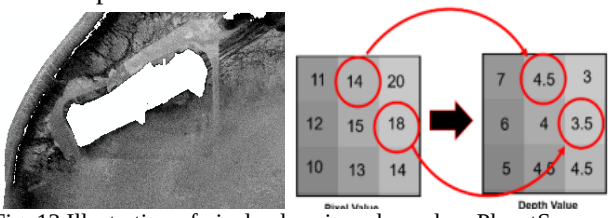


Fig. 12 Illustration of pixel values in a channel on PlanetScope; depth transformation based on pixel values predicted by statistical regression

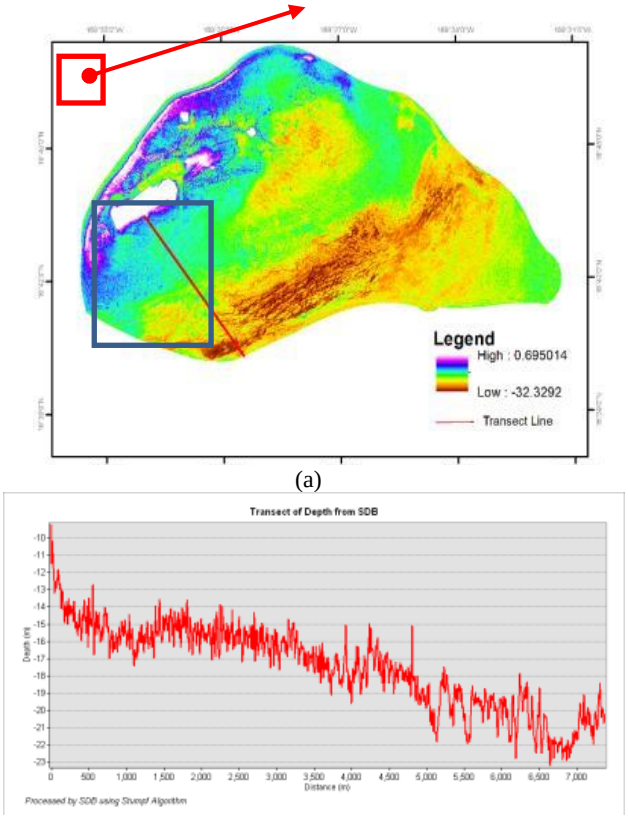


Fig. 13 Illustration of transect position in the study area (a); Transverse profile of depth obtained from SDB Stumpf method (b)

The second method used to obtain bathymetry information from satellite imagery is global regression analysis, also known as a global model. The satellite image data and tidal components used remain unchanged as before. In contrast to the algorithm developed by Stumpf [26] using band ratios, the global model method uses images simultaneously. Additionally, it uses the Ordinary Least Square (OLS) formula with the image data transformed in Eq. (11). Table 4 presents the ordinary least square statistical regression results in applying the global method in this study.

Table 4 Result of ordinary least square statistical regression

| Variable | Coefficient [a] | Intercept |
|---|---|---|
| Blue | 130.625000 | 2.046608 |
| Green | -354.358550 | |
| Red | -155.636474 | |
| Ratio Blue/Green | 16.112886 | |

The first result of SDB processing using a global method based on Ordinary Least Square regression in Johnston Atoll waters resulted in a depth ranging between 66.5074 and 26.8878 meters (in positive condition) (see Fig. 14a). The results were normalized to produce a more rational number, which represents the height in the intertidal area (-0.00002988) with water (0 - 66.5074 meters) (Fig. 14b). Furthermore, the numbers are set in a positive state to simplify calculations in the initial processing. It also represents the sample data taken as positive numbers (float). The processed bathymetry results were corrected with the high receding value (see Fig. 14c). The last process involves making the overall bathymetry value negative because it is below sea level (see Fig. 14d).

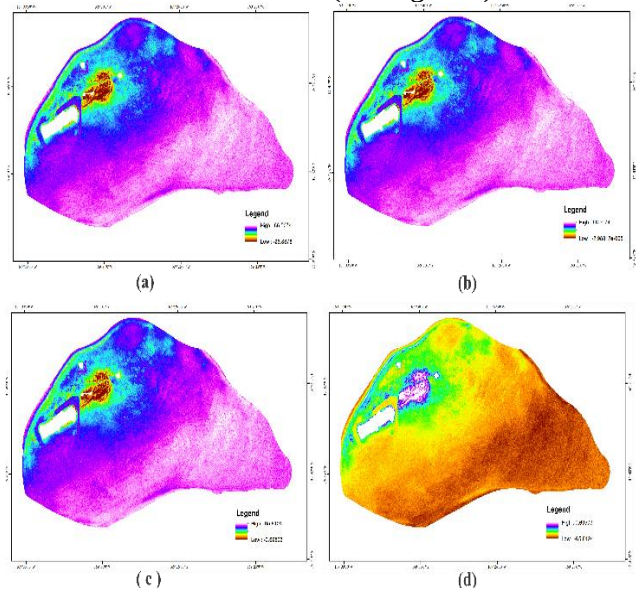


Fig. 14 Original results of SDB processing using the Global method (a); normalized SDB results (b); tide-corrected SDBs (c); SDB whose depth value has been adjusted to be below the water surface (minus) (d)

After being corrected by the reduction value, the maximum depth obtained through the global method reaches -65.8124 meters. However, this value is biased from the sample data used, and it is then cleared manually. Fig. 15 shows the depth distribution curve generated from the SDB process based on 3 x 3pixel dimensions according to the PlanetScope Image resolution. Additionally, the visual appearance on the histogram shows the data concentration ranging between -1 and 0 and between -40 and -10. These values are the basis for the masking process, removing only the depth value, including noise. After the removal, the resulting depth value ranges between -36 and 0 relative, close to the Stumpf method. Fig. 16 shows the masked SDB results and a depth profile taken from one of the Johnston Atoll waters transects.

Also, the transverse profile formed is similar to the one generated on the SDB transect using the Stumpf method [26].

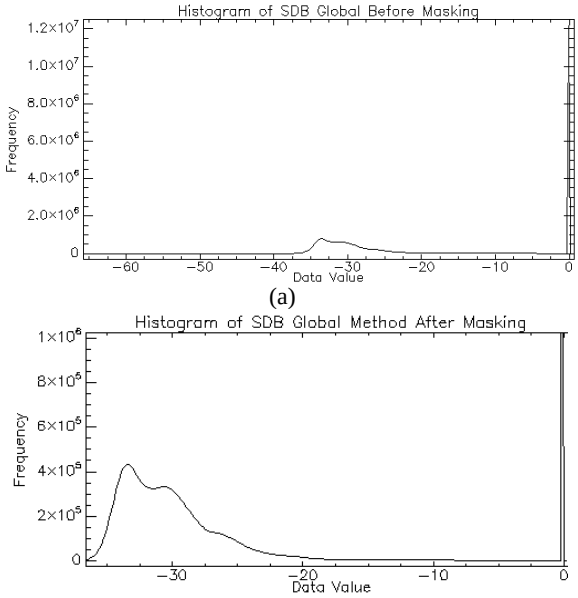


Fig. 15 Histogram before the masking process in selecting the depth value(a); Histogram after masking the depth value considered as noise (b)

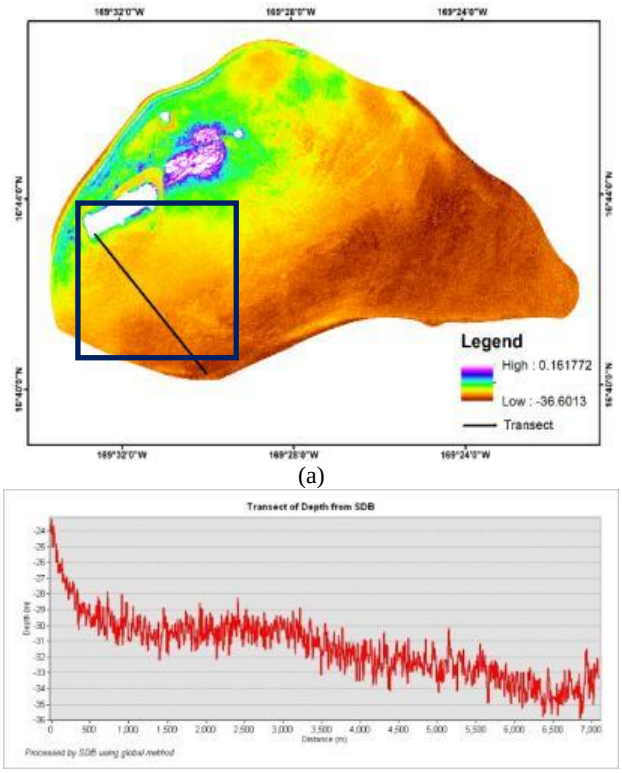


Fig. 16 Illustration of transect position in the study area (a); Transverse profile of the depth obtained from the SDB Global method (b)

The third method of obtaining bathymetric information is a single band/ratio adopted from Wicaksono [21]. The bands involved are blue, green, and log-transformed blue/green, with different correlation levels (Table 5). The blue/green log-transformed band had the strongest correlation and was processed into a bathymetric model. The linear regression results between the log-transformed blue/green band and the depth values were applied to obtain the original bathymetric model from the single-band method (see Fig. 17a). The next process involved normalizing the SDB data (Fig. 17b). Based on the single-band method, the depth range obtained experiences a tidal correction (Fig. 17c) of 2m (above the chart datum) to > 10m (below the chart datum) Fig. 17d). The resulting depth profile of the SDB processing using this method is illustrated in Fig. 18.

Table 5 Determinant value ($r^2$) and correlation ($r$) of single-band pixel value with depth

| **Band** | **$R^2$** | **r** | **Band** |
|---|---|---|---|
| Blue | 0.099 | 0.31 | Blue |
| Green | 0.0043 | 0.65 | Green |
| Ln (Blue/Green) | 0.681 | 0.82 | Ln (Blue/Green) |

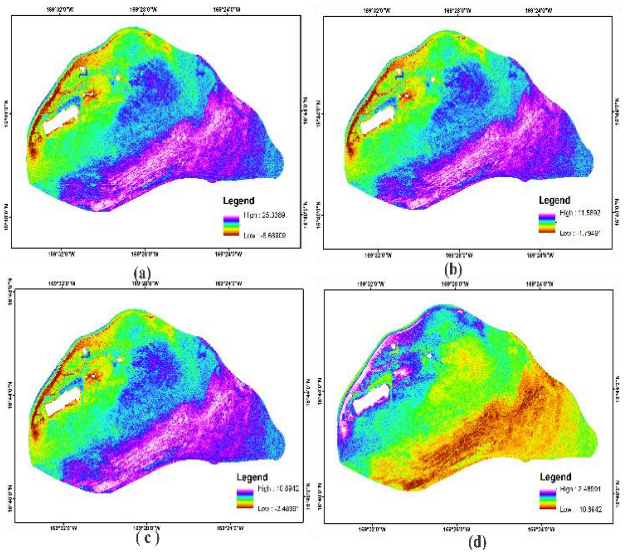


Fig. 17 The original SDB processing results using the single band method (a); the normalized SDB results (b); SDB after tidal correction (c); SDB after adjusting the depth adjustment to below the water level (minus) (d)

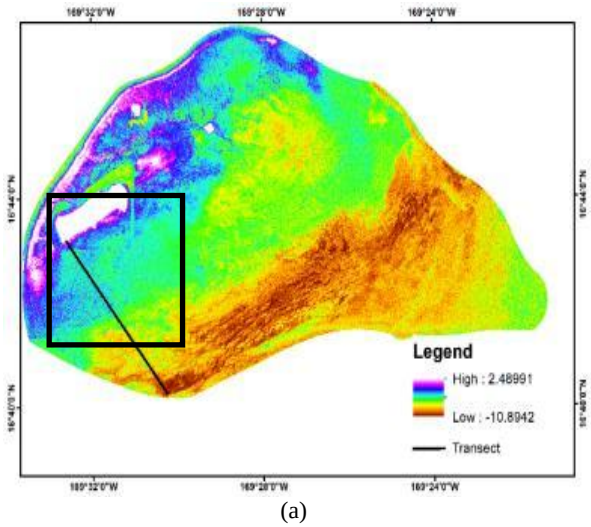

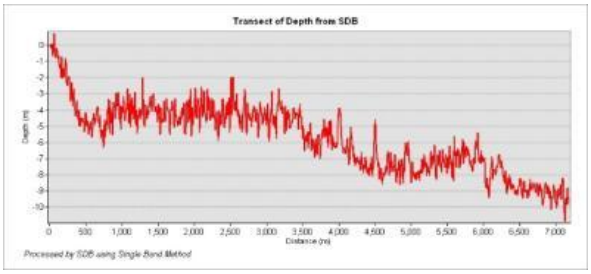


(b)

Fig. 18 Illustration of transect position in the study area (a); Transverse profile of depth obtained from SDB Single Band method (b)

### 3.3. Validation

The depth of the SDB processing data needs validation using the correct data. Validation and sample data considered correct are obtained from the NOAA marine map sheet number 83637. Therefore, validation is necessary to determine the estimated accuracy that could be accommodated and the precision obtained (RMSE; equation 12) [5, 24, 1].

$$RMSE = \sqrt{\sum_{i=0}^{n} \frac{(chart\ depth - model\ depth)^2}{n}} \qquad (12)$$

The RMSE accuracy values are calculated in three depth classes of data validation, 0-5, 5.01-10, and 10.01-20 meters, as shown in Table 6. Tests were only carried out on these three classes to provide limitations in the depth validation.

Table 6 RMSE based on depth class and SDB method

| | Stumpf | | | Global | | | Single Band | | |
|---|---|---|---|---|---|---|---|---|---|
| | 0-5 | 5-10 | 10-20 | 0-5 | 5-10 | 1 0-20 | 0-5 | 5 0-10 | 1 0-20 |
| RMSE (±) | 3.7 | 2.9 | 2.0 | 4.9 | 4.6 | 4.1 | 1.5 | 1.9 | 3.03 |

### 3.4. Total Vertical Uncertainty

The bathymetric information obtained from the SDB extraction method is not fully applicable to certain thematic activities. For this reason, the accuracy recommended by IHO based on S-44 refers to TVU (Total Vertical Uncertainty). Based on the depth range of 0 to 20 meters, the accuracy test is divided into 0 - 5, 5.01 - 10, and 10.01 - 20 meters. Additionally, TVU is described according to the SDB method used. The TVU calculations results for each method applied are presented in Tables 7-9.

Table 7 TVU values for SDB using the Stumpf method

| Depth | Sample total | Order | | | Not applicable | RMSE |
|---|---|---|---|---|---|---|
| | | Special | 1A/1B | 2 | | |
| 0-5 | | 0 | 0 | 0 | 100% | 3.7 |
| 5,01-10 | 103 | 0 | 0 | 0 | 100% | 2.9 |
| 10,01-20 | | 6,8% | 3,9% | 8,7% | 80,6% | 2.0 |

Table 8 TVU value for SDB using the Global method

| Depth | Sample Total | Order | | | Not Applicable | RMSE |
|---|---|---|---|---|---|---|
| | | Special | 1A/1B | 2 | | |
| 0-5 | | 0 | 0 | 0 | 100% | 4.9 |
| 5,01-10 | 103 | 0 | 0 | 0 | 100% | 4.6 |
| 10,01-20 | | 0% | 0% | 0% | 100% | 4.1 |

Table 9 TVU value for SDB using single band method

| Depth | Sample total | Order | | | Not applicable | RMSE |
|---|---|---|---|---|---|---|
| | | Special | 1A/1B | 2 | | |
| 0-5 | | 16.5% | 3.9% | 7.8 % | 71.8% | 1.5 |
| 5,01-10 | 103 | 4.9% | 6.8% | 4.9 % | 83.5% | 1.9 |
| 10,01-20 | | 0% | 0% | 0% | 100% | 3.03 |

## 4. Discussion

The bathymetry information from PlanetScope satellite imagery assisted by NOAA Nautical Chart for depth figures was reduced using the Stumpf *et al.* [26] approach, global model, and Single-band method. The three methods used simple statistical regression in the developed operating algorithm on the same sample. The depth range generated from the three methods produces fluctuating information. The Stumpf method [26] obtained depth data ranging between 0 and 32 meters; the global method produces 0 to 36 meters, while the single band method produces 2 to 10 meters below sea level.

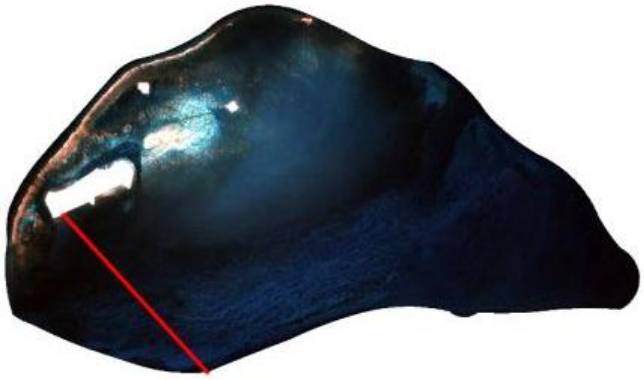

(a)

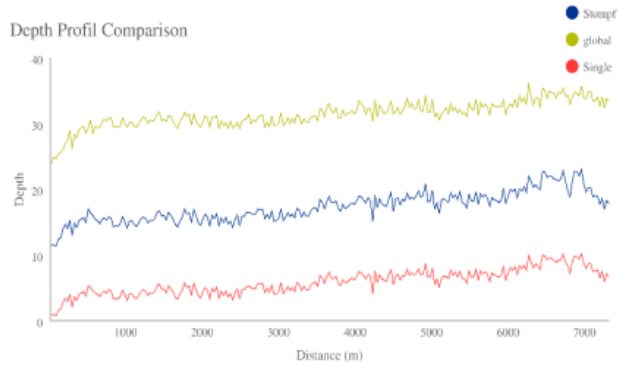


(b)

Fig. 19 Illustration of transect position in the study area (a); Cross-sectional profile of the SDB generated by the three methods (b)

The RMSE calculation results show that the best

value for the depth range of 0 to 5 meters and 5.01 to 10 meters are found in the single band method. Furthermore, the depth range of 10.01 to 20 meters with the best RMSE is found in the Stumpf method [26]. Observations show that the RMSE value decreases systematically with an increase in depth of the Stumpf [26] method and the global model. Also, the RMSE value is greater in the single band method due to the deeper studied waters. According to Bierwirth and Burne [16], light entering the water column is absorbed and scattered by water and the bottom substrate.

Additionally, the light energy attenuation increases with increasing depth due to absorption by water molecules, solutes, or particles. Therefore, the SDB depth value results in inaccuracy due to the water column bias causing a deeper depth range, increasing the theoretical RMSE value under the RMSE value generated by the single band method.

The resulting depth variation for the three methods is also quite far. Depth samples taken by transect (cross-bathymetry profile) show different depth ranges for the same location (Fig. 19). Furthermore, the results of the calculation of TVU from the three methods cannot reach the standard set by IHO – S44. Stumpf et al. [26] was the only method covering <20% of the TVU classification for a depth range of 10.01 to 20 of the total sample. Therefore, it is not yet applicable to the standard navigation requirements of the IHO. Similarly, the global method of the whole sample is not eligible for inclusion in the TVU classification according to the IHO standard, which is 95% of all uncertainty confidence levels.

Moreover, the single band method only covered 28.2% of the total sample in the 0-5 meters depth range and 16.5% in the 5.01-10 meters range. In contrast, better results are shown by SDB using the single band method. PlanetScope image data has technical weaknesses, including on the radiometric side of the image due to the low signal-to-noise ratio (SNR) [25] due to the significant effect of statistical regression on the depth results obtained based on the SDB in the Johnston Atoll Island waters using PlanetScope imagery.

## 5. Conclusion

This study focuses on acquiring SDB data based on three empirical statistical methods, namely the Global, Stumpf, and Single Methods. The scope of the study area is the optically shallow water around Johnston Atoll. The selection of the method was based on the proprietary NOAA nautical chart data source number 83637 plan B. The empirical method has the advantage that the attenuation capability at each depth sample point is the same so that the results of the regression calculations can be applied to all images. The color of the water that appears in the image at the recording time looks quite bright and clear, so there is no need for other interventions in the processing process. With a depth range of 0.9 - 20 meters, the waters around the optically shallow sea of Johnston Atoll appear clear, making it suitable for use as an SDB pilot location. The use of TVU as a new approach in seeing the accuracy of SDB results is an implementation of the standardization set by IHO through S-44 and other statistical-based methods. The satellite image used is PlanetScope which has been operating since 2017, so it is a new player in the range of multispectral satellite imagery. Through the SDB results, it can be seen that the three methods used produce different depth patterns. The resulting difference in depth pattern is the result of differences in the ability of the image to respond to the formula used.

The single band method produces better RMSE and TVU values than the three methods used. The RMSE pattern shows that the single band method aligns with the theory of light radiation to the waters. The theory states that the deeper the depth value, the more the RMSE value. Moreover, the depth variation in the three methods used shows a significant difference at one depth location. Based on TVU's calculations, the three SDB methods used, Stumpf [26], global, and single-band, have not reached the IHO – S44 standard of 95% confidence level. Accuracy based on the resulting TVU is 19.4% collectively (Special Order: 6.8% Order 1A/1B: 3.9% and order 2: 8.7%) for the depth range of 10.01 – 20 meters on the Stumpf method [26]. The accuracy is at 28.2% collectively in the single band method (Special Order: 16.5% Order 1A/1B: 3.9% and Order 2: 7.8%) for the 0-5 depth range and 16.5% collective order (Special Order: 4.9% Order 1A/1B: 6.8% and order 2: 4.9%) for the depth range of 5.01 – 10 meters. The Global Method cannot produce depths that fall into the order category based on the TVU classification. It should be noted, in general, based on the analysis of the accuracy of the SDB, it has technical weaknesses and is supported by the advantages of its good spatial resolution (3.5m). The weakness is in the radiometric side of the image due to the low signal-to-noise ratio because of the significant effect of statistical regression on the depth results obtained based on the SDB in the Johnston Atoll Island waters using PlanetScope imagery.

## Acknowledgments

All authors had equal contributions to this study. The authors declare that they have no known competing financial interests or personal relationships that could have influenced the work reported in this paper. Processing and analysis were carried out at the Marine and Coastal Data Laboratory, Marine Research Center, Ministry of Marine Affairs and Fisheries (KKP) of the Republic of Indonesia. Also, they were performed at the Hydro-Oceanography Laboratory of The Indonesia Naval Postgraduate School (STTAL), Jakarta, Indonesia. This article's publication was

funded by STTAL for the research project "Development of a Fusion-Oceanographic System Prototype for the Development of the Maritime Sector" for the 2021 fiscal year.

## References

[1] MUZIRAFUTI A., BARRECA G., CRUPI A., FAINA G., PALTRINIERI D., LANZA S., and RANDAZZO G. The Contribution of Multispectral Satellite Image to Shallow Water Bathymetry Mapping on the Coast of Misano Adriatico, Italy. *Journal of Marine Science and Engineering*, 2020, 8(2): 1-21. https://doi.org/10.3390/jmse8020126

[2] SAID C.N., MAHMUD M.R., and HASAN R.C. Evaluating satellite-derived bathymetry accuracy from Sentinel-2A high-resolution multispectral imageries for shallow water hydrographic mapping evaluating satellite-derived bathymetry accuracy. *IOP Conference Series: Earth and Environmental Science*, 2018: 1-9.

[3] EL-DIASTY M. Satellite-based bathymetric modeling using a wavelet network model. *ISPRS International Journal of Geo-Information*, 2019, 8(9): 1-14. https://doi.org/10.3390/ijgi8090405

[4] MISRA A., and RAMAKRISHNAN B. Assessment of coastal geomorphological changes using multi-temporal. *Continental Shelf Research*, 2020, 207(7): 1-16. https://doi.org/10.1016/j.csr.2020.104213

[5] MANESSA M.D.M., KANNO A., SEKINE M., HAIDAR M., YAMAMOTO K., IMAI T., and HIGUCHI T. Satellite-Derived Bathymetry Using Random Forest Algorithm and Worldview-2 Imagery Geoplanning. *Journal of Geomatics and Planning*, 2016, 3(2): 117-126. https://doi.org/10.14710/geoplanning.3.2.117-126

[6] CASAL G., MONTEYS X., HEDLEY J., HARRIS, P., CAHALANE C., and MCCARTHY T. Assessment of empirical algorithms for bathymetry extraction using Sentinel-2 data. *GIScience and Remote Sensing*, 2019, 40(8). https://doi.org/10.1080/01431161.2018.1533660

[7] KURNIAWAN A., and SANTOSO A.I. Obtaining low water line contour value for enclave claim regime 12 nautical miles on the Hatohobei Island Republic of Palau against the Republic of Indonesia according to UNCLOS 1982 using satellite-derived bathymetry. *IOP Conference Series: Earth and Environmental Science*, 2019, 389(1). https://doi.org/10.1088/1755-1315/389/1/012028

[8] CHYBICKI A. Three-Dimensional Geographically Weighted Inverse Regression (3GWR) Model for Satellite-Derived Bathymetry Using Sentinel-2 Observations. *Marine Geodesy*, 2018, 41(1): 1-23. https://doi.org/10.1080/01490419.2017.1373173

[9] LEDER T.D., LEDER N., and PEROŠ J. Satellite-derived bathymetry survey method – Example of Hramina bay. *Transactions on Maritime Science*, 2019, 8(1): 99-108. https://doi.org/10.7225/toms.v08.n01.010

[10] LOBEL P.S., LOBEL L.K., and RANDALL J.E. Johnston atoll: Reef fish hybrid zone between Hawaii and the equatorial pacific. *Diversity*, 2020, 12(2): 1-15. https://doi.org/10.3390/d12020083

[11] MELIALA L., WIBOWO W.A., and AMALIA J. Satellite-Derived Bathymetry on Shallow Reef Platform : A Preliminary Result from Semak Daun, Seribu Islands, Java Sea, Indonesia. In: *The 1st International Conference on Geodesy, Geomatics, and Land Administration, KnE Engineering*, 2019: 191-202. https://doi.org/10.18502/keg.v4i3.5849

[12] CASAL G., HARRIS P., MONTEYS X., HEDLEY J., CAHALANE C., and MCCARTHY T. Understanding satellite-derived bathymetry using Sentinel 2 imagery and spatial prediction models. *GIScience and Remote Sensing*, 2019, 57(3): 271-286. https://doi.org/10.1080/15481603.2019.1685198

[13] UNITED KINGDOM HYDROGRAPHIC OFFICE. *CSPCWG is invited to consider standardization and guidance for representing Satellite-Derived Bathymetry (SDB) data on paper charts and ENCs*. 11th CSPWG Meeting. Monaco: International Hydrographic Organization, 2015: 1-10.

[14] IHO. *International Hydrographic Organization Standards for Hydrographic Surveys S-44*. 6th ed. Monaco, International Hydrographic Organization, 2020.

[15] FREIRE R.R. *Evaluating Satellite-Derived Bathymetry Regarding Total Propagated Uncertainty, Multi-Temporal Change Detection, and Multiple Non-Linear Estimation*. Doctoral Dissertation. University of New Hampshire, Durham, 2017. https://scholars.unh.edu/dissertation/2281

[16] BIERWIRTH P.N., LEE T.J., and BURNE R.V. Shallow sea-floor reflectance and water depth derived by unmixing multispectral imagery. *Photogrammetric Engineering & Remote Sensing*, 1993, 59(3): 331-338.

[17] KURNIAWAN A., and SANTOSO A.I. Obtaining low water line contour value for enclave claim regime 12 nautical miles on the Hatohobei Island Republic of Palau against the Republic of Indonesia following UNCLOS 1982 using satellite-derived bathymetry. *IOP Conference Series: Earth and Environmental Science*, 389(1): 1755-1315. https://doi.org/10.1088/1755-1315/389/1/012028

[18] PATTANAIK A., SAHU K., and BHUTIYANI M.R. Estimation of Shallow Water Bathymetry Using IRS-Multispectral Imagery of Odisha Coast, India. *Aquatic Procedia*, 2015, 4(6): 173-181. https://doi.org/10.1016/j.aqpro.2015.02.024

[19] PLANET. *Planet Imagery Product Specifications*. Planet Labs Inc., 2019.

[20] WICAKSONO P., and LAZUARDI. Assessment of PlanetScope images for benthic habitat and seagrass species mapping in a complex optically shallow water environment. *International Journal of Remote Sensing*, 2019, 39(17): 5739-5765. https://doi.org/10.1080/01431161.2018.1506951

[21] GABR B., AHMED M., and MARMOUSH Y. PlanetScope and Landsat eight imageries for bathymetry mapping. *Journal of Marine Science and Engineering*, 2020, 8(2): 1-17. https://doi.org/10.3390/jmse8020143

[22] WISHA J.A., TANTO T.A., PRANOWO W.S., and HUSRIN, S. Current movement in Benoa Bay water, Bali, Indonesia: Pattern of tidal current changes simulated for the condition before, during, and after reclamation. *Regional Studies in Marine Science*, 2018, 18: 177-187. https://doi.org/10.1016/j.rsma.2017.10.006

[23] MA, Y., XU, N., LIU, Z., YANG B., YANG F., WANG X.H., and LI S. Satellite-derived bathymetry using the ICESat-2 lidar and Sentinel-2 imagery datasets. *Remote Sensing of Environment*, 2020, 250, 112047. https://doi.org/10.1016/j.rse.2020.112047

[24] Vinayaraj P., Raghavan V., and Masumoto S. Satellite-

Derived Bathymetry using Adaptive Geographically Weighted Regression Model. *Marine Geodesy*, 2016, 39(6): 458-478.
https://doi.org/10.1080/01490419.2016.1245227
[25] WULANDARI S. A., and WICAKSONO P. Bathymetry mapping using PlanetScope imagery on Kemujan Island, Karimunjawa, Indonesia. *IOP Conference Series: Earth and Environmental Science*, 2021, 686(1): 1-12.
https://doi.org/10.1088/1755-1315/686/1/012032
[26] STUMPF R. P., HOLDERIED K., and SINCLAIR M. Determination of water depth with high resolution satellite imagery over variable bottom types. *Limnology and Oceanography*, 2003, 48: 547–556. https://doi.org/10.4319/lo.2003.48.1_part_2.0547
[27] JUPP D. L. B. Background and extensions to depth of penetration (DOP) mapping in shallow coastal waters. Proceedings of the Symposium on Remote Sensing of the Coastal Zone, Gold Coast, 1988, IV.2.1-IV.2.19.
[28] TIDES & CURRENTS. *Harmonic Constituents for 1619000, Johnston Atoll United States of America*, n.d. https://tidesandcurrents.noaa.gov/harcon.html?id=1619000

**參考文:**

[1] MUZIRAFUTI A.、BARRECA G.、CRUPI A.、FAINA G.、PALTRINIERI D.、LANZA S.、和 RANDAZZO G. 多光譜衛星圖像對意大利米薩諾亞得里亞蒂科海岸淺水測繪的貢獻。海洋科學與工程學報, 2020, 8(2): 1-21. https://doi.org/10.3390/jmse8020126
[2] SAID C.N.、MAHMUD M.R. 和 HASAN R.C.從哨兵-2A 高分辨率多光譜圖像評估衛星測深精度，用於評估衛星測深精度的淺水水文測繪。 物理研究所 會議系列：地球與環境科學，2018：1-9。
[3] EL-DIASTY M. 使用小波網絡模型的基於衛星的測深建模。國際攝影測量與遙感學會國際地理信息雜誌, 2019, 8(9): 1-14. https://doi.org/10.3390/ijgi8090405
[4] MISRA A., 和 RAMAKRISHNAN B. 使用多時相評估海岸地貌變化。大陸架研究, 2020, 207(7): 1-16.
https://doi.org/10.1016/j.csr.2020.104213
[5] MANESSA M.D.M.、KANNO A.、SEKINE M.、HAIDAR M.、YAMAMOTO K.、IMAI T.、和 HIGUCHI T. 使用隨機森林算法和世界觀-2 圖像地理規劃的衛星測深。測繪與規劃學報, 2016, 3(2): 117-126.
https://doi.org/10.14710/geoplanning.3.2.117-126
[6] CASAL G.、MONTEYS X.、HEDLEY J.、HARRIS, P.、CAHALANE C. 和 MCCARTHY T. 評估使用 哨兵-2 數據進行水深提取的經驗算法。地理科學與遙感, 2019, 40(8)。
https://doi.org/10.1080/01431161.2018.1533660
[7] KURNIAWAN A., 和 SANTOSO A.I.根據 1982 年《聯合國海洋法公約》，使用衛星測深法獲得帕勞 HATOHOBEI 島共和國對印度尼西亞共和國 12 海裡的飛地索賠制度的低水線等值線值。 物理研究所 會議系列：地球與環境科學，2019，389(1)。
https://doi.org/10.1088/1755-1315/389/1/012028
[8] CHYBICKI A. 使用 哨兵-2 觀測的衛星測深的三維地理加權逆回歸模型。海洋大地測量學, 2018, 41(1): 1-23.
https://doi.org/10.1080/01490419.2017.1373173
[9] LEDER T.D., LEDER N., 和 PEROŠ J. 衛星測深測量方法 – 赫拉米納灣示例。海事科學彙刊, 2019, 8(1): 99-108.
https://doi.org/10.7225/toms.v08.n01.010
[10] LOBEL P.S.、LOBEL L.K. 和 RANDALL J.E. JOHNSTON 環礁：夏威夷和赤道太平洋之間的礁魚雜交區。多樣性，2020 年，12（2）：1-15。
https://doi.org/10.3390/d12020083
[11] MELIALA L.、WIBOWO W.A. 和 AMALIA J. 淺礁平台上的衛星測深：印度尼西亞爪哇海斯里布群島檢查葉子的初步結果。在：第一屆大地測量學、測繪學和土地管理國際會議，工程，2019：191-202。
https://doi.org/10.18502/keg.v4i3.5849
[12] CASAL G.、HARRIS P.、MONTEYS X.、HEDLEY J.、CAHALANE C. 和 MCCARTHY T. 使用 哨兵 2 圖像和空間預測模型了解衛星測深。 地理信息系統 科學與遙感，2019 年，57(3)：271-286。
https://doi.org/10.1080/15481603.2019.1685198
[13] 英國水文局。邀請海圖標準化和紙質海圖工作組考慮在紙質海圖和電子海圖上表示衛星測深數據的標準化和指導。第 11 次海圖標準化和紙質海圖工作組會議。摩納哥：國際水文組織。 2015：1-10。
[14] 國際衛生組織。國際水文組織水文測量標準 S-44。第 6 版。摩納哥，國際水文組織，2020 年。
[15] FREIRE R.R. 在總傳播不確定性、多時間變化檢測和多非線性估計方面評估衛星測深。博士論文。新罕布什爾大學，達勒姆，2017。
https://scholars.unh.edu/dissertation/2281
[16] BIERWIRTH P.N.、LEE T.J. 和 BURNE R.V.通過分解多光譜圖像得出的淺海底反射率和水深。攝影測量工程與遙感, 1993, 59(3): 331-338。
[17] KURNIAWAN A., 和 SANTOSO A.I.在 1982 年《聯合國海洋法公約》之後，使用衛星測深法獲得了帕勞哈托霍貝島共和國對印度尼西亞共和國 12 海裡的飛地索賠制度的低水線等值線值。 物理研究所 會議系列：地球與環境科學，389（1）：1755-1315。
https://doi.org/10.1088/1755-1315/389/1/012028
[18] PATTANAIK A.、SAHU K. 和 BHUTIYANI M.R. 使用印度奧里薩邦海岸的紅外線的多光譜圖像估計淺水深度。水生過程, 2015, 4(6): 173-181。
https://doi.org/10.1016/j.aqpro.2015.02.024
[19] 星球。行星圖像產品規格。行星實驗室公司，2019 年。
[20] WICAKSONO P., 和 LAZUARDI。在復雜的光學淺水環境中評估底栖栖息地和海草物種測繪的 星球範圍 圖像。國際遙感雜誌, 2019, 39(17): 5739-5765.
https://doi.org/10.1080/01431161.2018.1506951
[21] GABR B.、AHMED M.、和 MARMOUSH Y. 星球範圍 和陸地衛星用於測深測繪的八幅圖像。海洋科學與工程學報, 2020, 8(2): 1-17.
https://doi.org/10.3390/jmse8020143
[22] WISHA J.A.、TANTO T.A.、PRANOWO W.S. 和 HUSRIN, S. 印度尼西亞巴厘島貝諾阿灣水域的海流運動：模擬開墾前、開墾期間和開墾後條件的潮流變化模式。海洋科學區域研究，2018, 18: 177-187. https://doi.org/10.1016/j.rsma.2017.10.006

[23] MA, Y., XU, N., LIU, Z., YANG B., YANG F., WANG X.H., 和 LI S. 使用 冰、雲和陸地高程衛星-2 激光雷達和哨兵-2 圖像數據集的衛星測深。環境遙感，2020, 250, 112047。
https://doi.org/10.1016/j.rse.2020.112047
[24] VINAYARAJ P.、RAGHAVAN V. 和 MASUMOTO S. 使用自適應地理加權回歸模型的衛星測深。海洋大地測量學, 2016, 39(6): 458-478。
https://doi.org/10.1080/01490419.2016.1245227
[25] WULANDARI S. A. 和 WICAKSONO P. 在印度尼西亞卡里蒙賈瓦的克木揚島上使用 星球範圍 圖像進行測深測繪。 物理研究所 會議系列：地球與環境科學，2021 年，686（1）：1-12。
https://doi.org/10.1088/1755-1315/686/1/012032
[26] STUMPF R. P.、HOLDERIED K. 和 SINCLAIR M. 使用高分辨率卫星图像在可变底部类型上确定水深。 湖沼学和海洋学，2003，48：547-556。
https://doi.org/10.4319/lo.2003.48.1_part_2.0547
[27] JUPP D. L. B. 背景和延伸到浅海沿岸深度 (DOP) 测绘。 海岸带遥感研讨会论文集，黄金海岸，1988 年，IV.2.1-IV.2.19。
[28] 潮流与潮流。 1619000 的谐波成分，美国约翰斯顿环礁，未注明日期。
https://tidesandcurrents.noaa.gov/harcon.html?id=1619000